JOURNAL OF THE KOREAN ASTRONOMICAL SOCIETY
30: 13 ~ 25, 1997

COMPARISON OF SOBOLEV APPROXIMATION WITH THE EXACT ALI IN P CYGNI TYPE PROFILE

CHOE, SEUNG-URN AND KO, MI-JUNG
Department of Earth Sciences, Seoul National University, Seoul 151-742, Korea
(Received Mar. 6, 1997; Accepted Apr. 1, 1997)

ABSTRACT

Sobolev approximation can be adopted to a macroscopic supersonic motion comparatively larger than a random (thermal) one. It has recently been applied not only to the winds of hot early type stars, but also to envelopes of late type giants and/or supergiants. However, since the ratio of wind velocity to stochastic one* is comparatively small in the winds of these stars, the condition for applying the Sobolev approximation is not fulfilled any more. Therefore the validity of the Sobolev approximation must be checked.

We have calculated exact P Cygni profiles with various velocity ratios, V_∞/V_{sto}, using the accelerated lambda iteration method, comparing with those obtained by the Sobolev approximation. While the velocity ratio decrease, serious deviations have been occured over the whole line profile. When the gradual increase in the velocity structure happens near the surface of star, the amount of deviations become more serious even at the high velocity ratios. The investigations have been applied to observed UV line profile of CIV in the Copernicus spectrums of ζ Puppis and NV of τ Sco. In case of τ Sco which has an expanding envelope with the gradual velocity increase in the inner region, The Sobolev approximation has given the serious deviations in the line profiles.

Key Words : P Cygni profile, radiative transfer, Sobolev approximation, Accelerated lambda Iteration

I. INTRODUCTION

Since the UV spectral region became accessible through extra-terrestrial observations, the phenomena of mass loss and stellar winds have attracted growing interest. Especially among the early-type stars an unexpected large number exhibit UV lines with so called P Cygni profiles (i.e. a redward displaced emission together with a blue-shifted absorption) as a consequence of expanding stellar atmospheres. The investigation of the observed P Cygni profiles, as a main source of information about these expanding envelopes, requires an adequate theory of spectral line formation. Supersonic wind velocities give a reason to apply the approximation of Sobolev which assumes that the random (thermal) motions can be neglected against the macroscopic flow velocities. Castor(1970) used escape probabilities to calculate the line source function. This technique is originally based on the Sobolev approximation(Choe, *et al.*, 1996). It can be used on the assumption of supersonic wind. Neverthless, one has to depend on the Sobolev approximation not onle in supersonic cases but also in thermal velocity dominant cases, because complexity of the geometry make a numerical solution for the source function be very slow and uneconomical.

In this paper, exact line profiles are calculated by Accelerated Lambda Iteration (hereafter abbreviated ALI) and

* Stochastic velocity involves both thermal velocity and microturbulent velocity.

$$V_{sto} = \sqrt{{V_{th}}^2 + {V_{turb}}^2}$$

compared with those which have been calculated through Sobolev approximation at various velocity ratios, V_∞/V_{sto}. This investigation is extended to observed doublets. This is of practical imfortance because most of the observed UV lines appear as overlapping doublets.

The transfer equation is formally solved using a Feautrier scheme in the observer's frame with specific numerical features as described by Rybicki & Hummer (1991). The ALI procedure has been developed by Robert Baade. This code has used a tridiagonal approximate lambda operator constructed via integral representation of the transfer equation.

In Section II, theories which are used in the computer code are given. In Section III, the parameters used in this study are given. In Section IV, for a representative set of parameters the results of ALI and Sobolev approximation are compared and discussed. In Section V, a fit of two observed UV resonance doublets is performed. In Section VI, some conclusions are discussed.

II. THEORY

The transfer equation for a two-level atom in a three-dimensional moving medium has been discussed in detail by Rybicki and Hummer(1978). It can be written

$$\vec{n}\cdot\nabla I(\vec{r},\vec{n},\nu) = -\kappa(\vec{r})\phi[\nu - \frac{\nu_0}{c}\vec{n}\cdot\vec{v}(\vec{r})][I-S] \tag{1}$$

$I(\vec{r},\vec{n},\nu)$ is the specific intensity at point $\vec{r}$ in direction defined by the unity vector $\vec{n}$ and at frequency ν, and $\vec{v}(\vec{r})$ is the material velocity field. The quantity

$$\kappa(\vec{r}) = \frac{h\nu_0}{4\pi}B_{12}n_k(\vec{r}) \tag{2}$$

is the integrated line opacity, where ν_0 is the line-center frequency, B_{12} is the Einstein coefficient, and n_k is the population of the lower level. The line profile function $\phi(\vec{r},\nu)$ has the frequency normalization

$$\int_0^\infty \phi(\vec{r},\nu)d\nu = 1 \tag{3}$$

It is difficult to find the formal solution of the radiative transfer equation in the moving medium. But using an appropriate condition the formal solution can be simplified. In case of the large velocity gradient in the medium, the Sobolev approximation can be used. When the velocity gradient in the medium are sufficiently large, the profile function ϕ in the eq(1) is typically very narrow, it behaves like δ -function. So that along a given ray the intensity at frequency ν does not change at all, except at certain discrete resonance points, where the material has just the right Doppler shift to allow it to absorb and emit at frequency ν. Therefore, the problem of determining the intensities reduces to the simpler one of determining the variation of intensity in the neighborhood of a single resonance point. This is the essence of the Sobolev approximation. Therefore we easily obtain the formal solution of the eq(1). Integrating it over frequency, we obtain the mean intensity, $\bar{J}(\vec{r})$. It can be written (Rybicki and Hummer, 1978)

$$\bar{J}(\vec{r}) = [1-\beta(\vec{r})]S(\vec{r}) + \beta_c(\vec{r})I_c \tag{4}$$

The quantities β and β_c are escape probabilities. They are given by

$$\beta(\vec{r}) = \frac{1}{4\pi}\int d\Omega\,\frac{1-e^{-\tau}}{\tau}\,, \qquad \beta_c(\vec{r}) = \frac{1}{4\pi}\int_{\Omega_c} d\Omega\,\frac{1-e^{-\tau}}{\tau} \tag{5}$$

For complete redistribution, the source function is

$$S(\vec{r}) = \frac{\bar{J}(\vec{r}) + \epsilon'(\vec{r})B_\nu(\vec{r})}{1+\epsilon'(\vec{r})} \tag{6}$$

where ϵ' is called by thermalization parameter. If $\epsilon' = 0$, then $S(\vec{r}) = \bar{J}(\vec{r})$ and if ϵ' becomes $\gg 1$, then $S\ (\ \vec{r}\ ) \longrightarrow B_\nu\ (\ \vec{r}\ )$. B_ν is the Planck function at frequency ν and local electron temperature at point $\vec{r}$. The source function can be determined by substituting eq(4) into eq(6)

$$S(\vec{r}) = \frac{\beta_c(\vec{r})I_c + \epsilon'(\vec{r})B_\nu(\vec{r})}{\epsilon'(\vec{r}) + \beta(\vec{r})} \tag{7}$$

In order to check the validity of the Sobolev approximation not only in supersonic cases but also non-supersonic one, numerical calculation must be done. ALI method is the most straightforward numerical method of solution of the equation of radiative transfer. This method can be adopted even to non-supersonic cases. ALI method is based on the use of an approximate Λ operator. In this paper, tridiagonal approximate Λ operator has been used(see Cannon, 1985). The spherical symmetry allow us treat a transfer equation with 1-dimensional problem. Therefore eq(1) can be rewrited:

$$\mu\frac{\partial I}{\partial \tau}(\tau, \triangle\nu, \mu) = \phi(\triangle\nu)\,[I(\tau, \triangle\nu, \mu) - S(\tau)] \tag{8}$$

where

$$\triangle\nu = \nu - \frac{\nu_o}{c}\vec{n}\cdot\vec{v}(\vec{r}) \tag{9}$$

Eq(8) may be immediately written in the form

$$I(\tau, \triangle\nu, \mu) = \int_\tau^\infty \phi(\triangle\nu)\,S(\tau')\,e^{-\phi(\triangle\nu)(\tau'-\tau)/\mu}\frac{d\tau'}{\mu} \tag{10}$$

for all $\mu > 0$ whilst, for $\mu < 0$, we have

$$I(\tau, \triangle\nu, \mu) = -\int_0^\tau \phi(\triangle\nu)\,S(\tau')\,e^{-\phi(\triangle\nu)(\tau'-\tau)/\mu}\frac{d\tau'}{\mu} \tag{11}$$

where we have taken zero incident radiation flux at the surface of the atmosphere. If we now substitute these expressions into the source function $S(\tau)$ given by eq(6) using the definition of the mean intensity, we find

$$\begin{aligned} S(\tau) =& \frac{1}{2(1+\epsilon')}\int_{-\infty}^{\infty}\phi(\triangle\nu)\,d(\triangle\nu)\times \\ & \left(\int_0^1\frac{d\mu}{\mu}\int_\tau^\infty d\tau' - \int_{-1}^0\frac{d\mu}{\mu}\int_0^\tau d\tau'\right)S(\tau')\phi(\triangle\nu)\,e^{\phi(\triangle\nu)(\tau'-\tau)/\mu} + \frac{\epsilon'}{1+\epsilon'}B_\nu \end{aligned} \tag{12}$$

Replacing μ by $-\mu$ in the second term in braces appearing in eq(12) then yields

$$\begin{aligned} S(\tau) =& \frac{1}{2(1+\epsilon')}\int_{-\infty}^{\infty}\phi(\triangle\nu)\,d(\triangle\nu)\times \\ & \int_0^1\frac{d\mu}{\mu}\int_0^\infty d\tau'\,S(\tau')\phi(\triangle\nu)e^{-\phi(\triangle\nu)|\tau'-\tau|/\mu} + \frac{\epsilon'}{1+\epsilon'}B_\nu \end{aligned} \tag{13}$$

which we rewrite as

$$S(\tau) = \frac{1}{1+\epsilon'}\Lambda S(\tau') + \frac{\epsilon'}{1+\epsilon'}B_\nu \tag{14}$$

where the operator Λ obviously has the form

$$\Lambda \equiv \frac{1}{2}\int_{-\infty}^{\infty}\phi^2(\triangle\nu)\,d(\triangle\nu)\int_0^1\frac{d\mu}{\mu}\int_0^\infty e^{-\phi(\triangle\nu)|\tau'-\tau|/\mu}d\tau' \tag{15}$$

The Λ iteration procedures then involve an initial guess at $S(\tau)$, substitution of this guess into the RHS of eq(14) to obtain a new $S(\tau)$, then resubstitution, etc, until convergence is attained. We therefore have the nth iteration term:

$$S_n = \frac{1}{1+\epsilon'}\Lambda S_{n-1} + \frac{\epsilon'}{1+\epsilon'}B_\nu \tag{16}$$

The convergence of the Λ iterative scheme is well explained in Cannon(1985).

III. THE PARAMETRIZATION

The absorption coefficient in eq(2), $\kappa(r)$, may also be written as

$$\kappa(r) = \frac{\pi e^2}{m_e c} f n_k(r) \phi(\nu) \tag{17}$$

where f is the oscillator strength, $n_k(r)$ is a number density of the absorbers, and ϕ is the profile function

$$\phi(\nu) = \frac{1}{\sqrt{\pi}\triangle\nu_D} e^{-(\nu-\nu_0)/\triangle\nu_D}$$

$$\int_0^\infty d\nu\, \phi(\nu) = 1$$

In this paper, the Doppler width, $\triangle\nu_D$, is used as the unit of frequency interval.

$$\triangle\nu_D = \frac{\nu_o}{c} V_{sto} \ , \qquad V_{sto} = \sqrt{{V_{th}}^2 + {V_{turb}}^2} \tag{18}$$

Introducing new dimensionless frequency variables, $\xi = \frac{\triangle\nu}{\triangle\nu_D}$, profile function becomes

$$\varphi(\xi) = \triangle\nu_D\, \phi(\xi\, \triangle\nu_D) \tag{19}$$

Therefore eq(17) becomes

$$\kappa(r) = \frac{\pi e^2}{m_e c} f n_k(r) \varphi(\xi) \frac{1}{\triangle\nu_D} \tag{20}$$

Defining that q is a weight function, describing the depth dependence of the degree of ionization, from the continuity equation

$$4\pi {R_c}^2 V(R_c) n_k(R_c) \frac{1}{q(R_c)} = 4\pi r^2 V(r) n_k(r) \frac{1}{q(r)} \tag{21}$$

where R_c is star radius. Therefore we obtain

$$n_k(r) = \frac{{R_c}^2 V(R_c) n_k(R_c) q(r)}{r^2 V(r) q(R_c)} \tag{22}$$

Substituting eq(22) into eq(20) then

$$\kappa(r) = \frac{\pi e^2}{m_e c} f \frac{{R_c}^2 V(R_c) n_k(R_c) q(r)}{r^2 V(r) q(R_c)} \frac{c}{\nu_0 V_{sto}} \tag{23}$$

For the computer calculation, we introduce dimensionless parameters :

$$\Gamma = \frac{V_\infty}{V_{sto}} \tag{24}$$

$$u(r) = \frac{V(r)}{V_{sto}} \tag{25}$$

$$r' = \frac{r}{R_c} \tag{26}$$

$$K = \kappa R_c \tag{27}$$

$$(note : \int K dr' = \int \kappa\, dr)$$

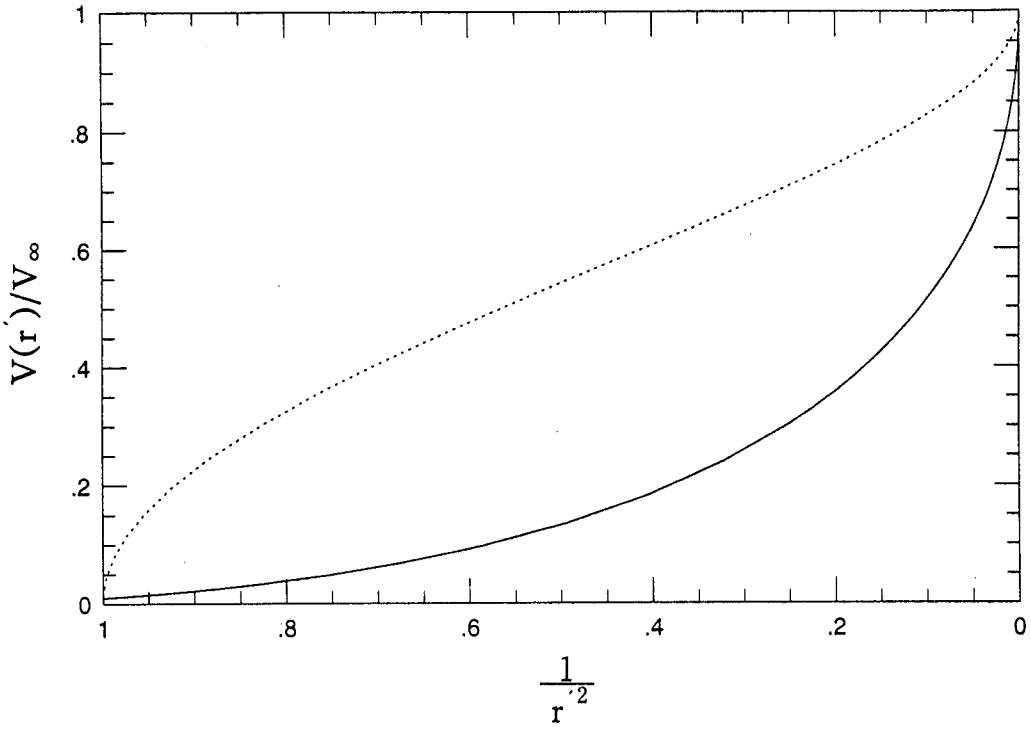

Fig. 1. velocity law for $\beta = 0.5$ (dashed line), $\beta = 2$ (solid line). r' is a radial distance from the center, normalized by R_c. For $\beta = 0.5$, $V(r)$ has a steep gradient near a surface of a star and it reaches quickly the terminal velocity, while the wind with $\beta = 2$ starts with a flat velocity gradient.

Finally we get

$$K = K_o \frac{1}{r'^2 u(r')} q(r') \Gamma^2 \varphi(\xi) \tag{28}$$

where

$$K_o = \frac{\pi e^2}{m_e c} f \lambda \frac{n_k(R_c)}{V_\infty} \frac{V(R_c)/V_\infty}{q(R_c)} R_c$$

For the velocity law we use the analytic expression

$$V(r) = V_\infty (1 - \frac{b}{r})^\beta \tag{29}$$

The value of b has been chosen such that $V(r) = 0.01 V_\infty$ at $r = R_c$. And V_∞ is terminal velocity of the wind. The parameter β is set either to 0.5 or 2. The $\beta = 0.5$ case corresponds roughly to the result of the stellar wind theory by Castor *et al.*(1975) and was often adopted in former investigations. This velocity law has a steep gradient near the photosphere and reaches the terminal velocity at small values of r. While the law with $\beta = 2$ starts with a very shallow gradient (see Figure 1).

IV. RESULTS AND DISCUSSION

(a)Comparison of the Sobolev Source Function with the Exact One

Figure 2 shows source functions that are calculated with both Sobolev approximation and ALI. For all Γ, the correct source functions start with large values ($S \approx I_c$) near the inner boundary, while the approximated source functions always start with $S = 0.5 I_c$ at $r = R_c$. This is the same result as that of Schönberg (1985). As he noted, this is due to geometrical reasons. The scattering surface, that is responsible for the value of the Sobolev

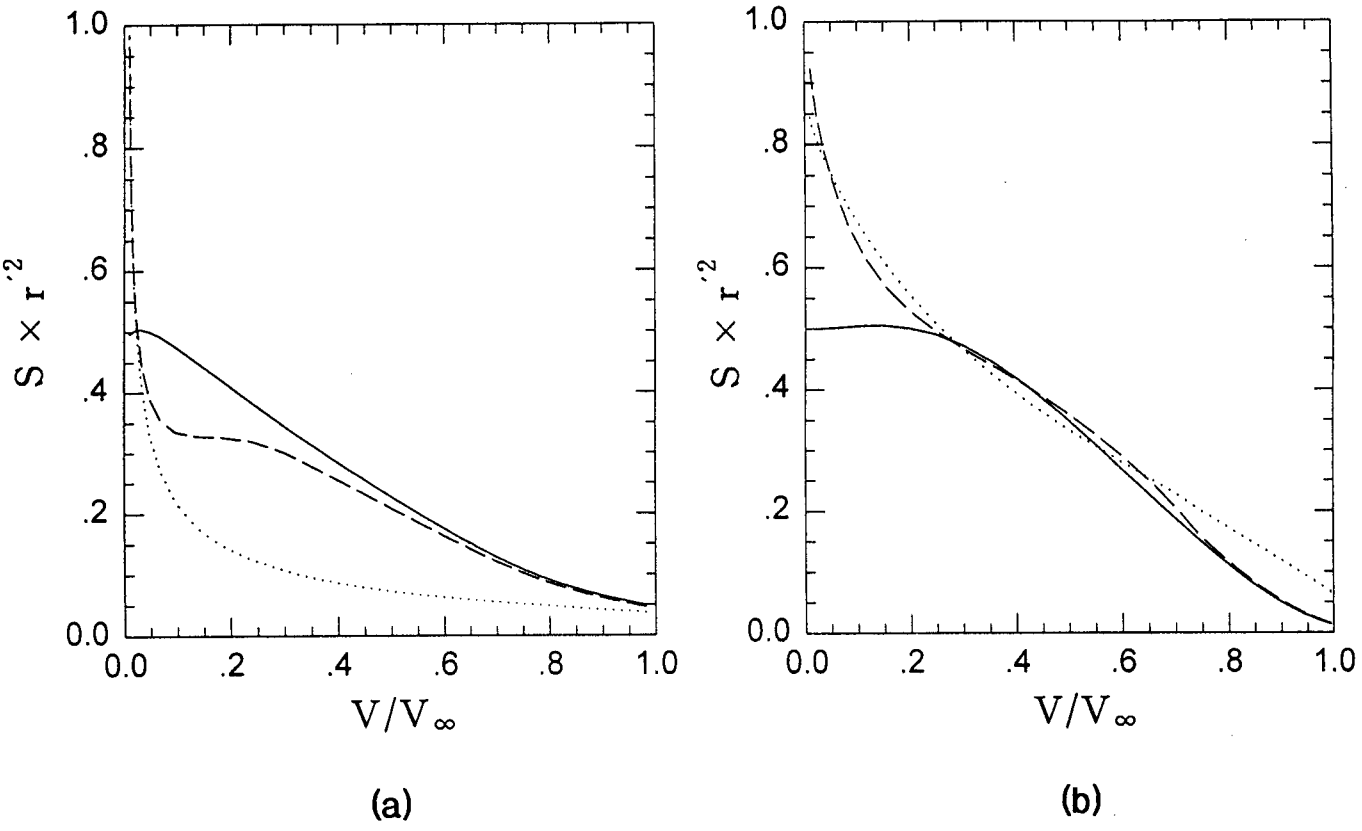

Fig. 2. Comparison of the Sobolev source function with that of ALI. Sobolev (solid line) at $\Gamma = 10$ and $\Gamma = 1$, ALI at $\Gamma = 10$ (dashed line), and ALI at $\Gamma = 1$ (dotted line). (a) with $K_o = 10, \beta = 2$; (b) with $K_o = 10, \beta = 0.5$

soure function at $r = R_c$, is attached to the surface of the opaque core. Therefore, any radiation back-scattered by envelope (this is calculated in escape probability β, see eq(5)) cannot come back by scattering. Only contribution to the source function at $r = R_c$ is the radiation coming directly from the core. But the real star surface is not opaque core. Most of the radiation is scattered here. Therefore correct source function S must start near the I_c.

In addition, for $\beta = 2$ in the outer parts of the envelope the exact source function is considerably smaller than the Sobolev source function. This is due to local computation in Sobolev approximation. Physical properties near the borders of the scattering zones may be completely different from the conditions in the center of the zones. If opacity gradient is steep, local computation will induce larger source function than exact source function. The reason is that a smaller value of the opacity than the real one overestimate the radiation from the core. The steeper opacity gradient, the discrepancy is larger. In Figure 3, we can see that opacity gradient for $\beta = 2$ is larger than that for $\beta = 0.5$ in $0 < \log r' < 0.4$. Therefore strong deviation is occured in source function for $\beta = 2$. And this deviation increase with decreasing Γ. Because the decrease of the value of Γ correspons to the increase of scattering zone. As you know, the validity of the Sobolev approximation depends on the spharpness of the resonance region.

(b) Comparison of the Sobolev Line Profile with the Exact One

The comparison is shown in Figure 4, 5, 6, 7. The calculated line profiles are much smoother than those in Choe, *et al.*(1996), because our code let the basic grid points be augmented automatically with a fine mesh to assure that the velocity jump between successive points is everywhere less than a pre-chosen value. At large Γ, the errors of the Sobolev approximation are considerably small. The small deviation has been occured within a few Doppler widths from the line center, λ_o, while in the outer part of line profiles the agreement with the exact line profiles

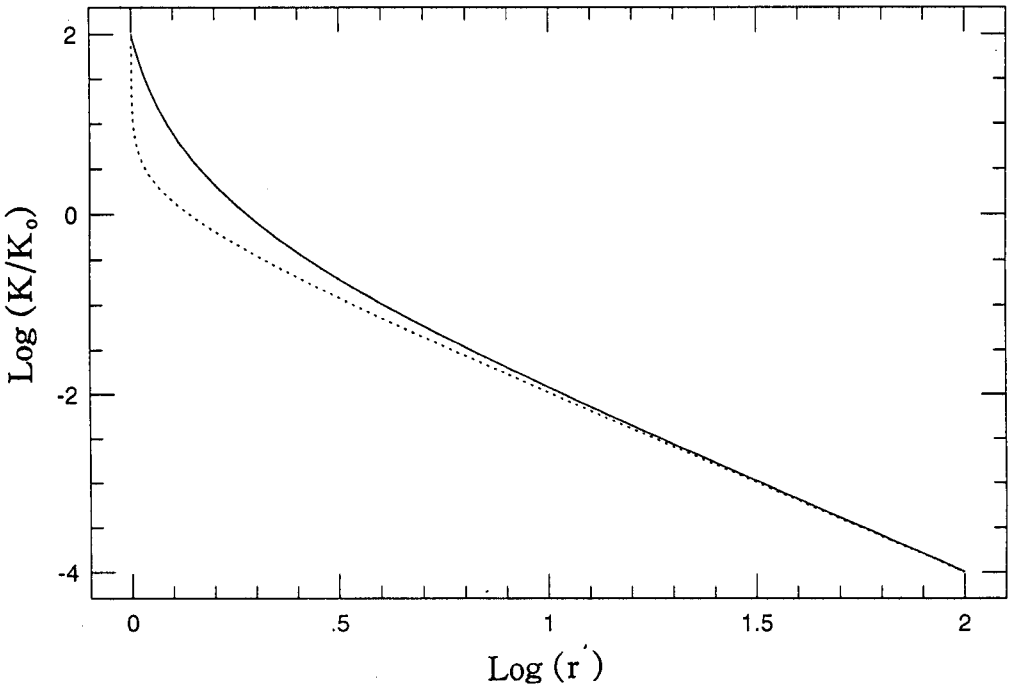

Fig. 3. Opacity function for $\beta = 0.5$ (dashed line), $\beta = 2$ (solid line).

is surprisingly good. Only at $\beta = 2$ considerable deviations occur (see Figure 4) This corresponds to the fact that small velocity gradients lead to extended resonance region. The larger K_o is , the larger are the errors of the Sobolev approximation. But, the influence of a opacity, K_o, is small (see Figure 5). At small Γ, the error extends over the whole line profiles. And the deviation with the exact line profiles is very serious. As at large Γ, $\beta = 2$ causes larger deviation than $\beta = 0.5$ (see Figure 6). And a large K_o causes larger deviations than a small K_o (see Figure 7). A comparison of the line profiles show that for a high velocity ratio the Sobolev approximation may be quite satisfactory except for $\beta = 2$. However, the Sobolev approximation should not be used for all case of a low velocity ratio.

V. FIT OF THE OBSERVED UV-LINE PROFILES

Since the UV spectral region became accessible through extraterrestrial observations, unexpected large number of UV lines with P Cygni type profiles have been found. Consequently there has been considerable interest in estimating the rate of mass ejection from various types of stars and understanding the driving mechanism, and so many alternative models have been proposed. The various models have their possibilities and difficulties. Obviously only further empirical work can decide between these alternative models. In order to interpret the observed P Cygni lines with a satisfactory model, a fit of observed line profiles is very necessary. We have investigated two ultraviolet resonance lines of CIV doublet of ζ Pup (Morton and Underhill, 1977) and NV doublet of τ Sco (Lamers and Rogerson, 1978). The CIV doublet of ζ Pup shows well-developed P Cygni profile. However, the NV doublet of τ Sco shows strong and asymmetric absorption line with faint P Cygni emission. Well developed P Cygni profiles indicate that the expanding envelope contains a large amount of material, corresponding to a high mass loss rate, and poorly developed P Cygni profiles with little emission indicate that the envelope contains a small amount of material, corresponding to a small mass loss rate (Lamers and Rogerson, 1978). Although the case of doublets is originally a multilevel problem, it has been treated with two 2-level atoms in this paper. Because the electron number density is low, about the order of $10^9 \lesssim n_e \lesssim 10^{12}$ in expanding envelope (Lamers and Morton, 1976), two excited levels which are the doublet components do not interact with each other via the rate equations. Therefore the treatment of two 2-level atoms is reasonable.

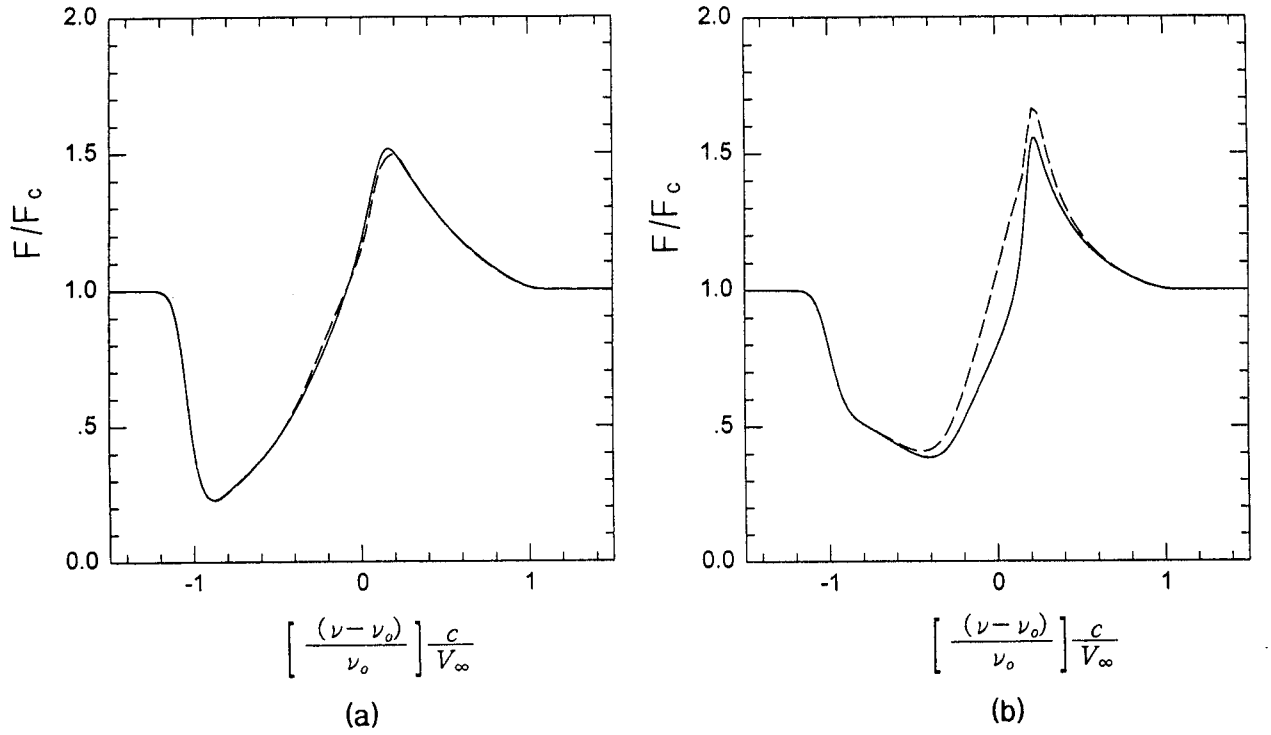

Fig. 4. Normalized flux profiles versus normalized frequency. Correct line profile (solid line), and Sobolev line profile (dashed line). (a) with $\Gamma = 10$, $K_o = 1$, $\beta = 0.5$; (b) with $\Gamma = 10$, $K_o = 1$, $\beta = 2$.

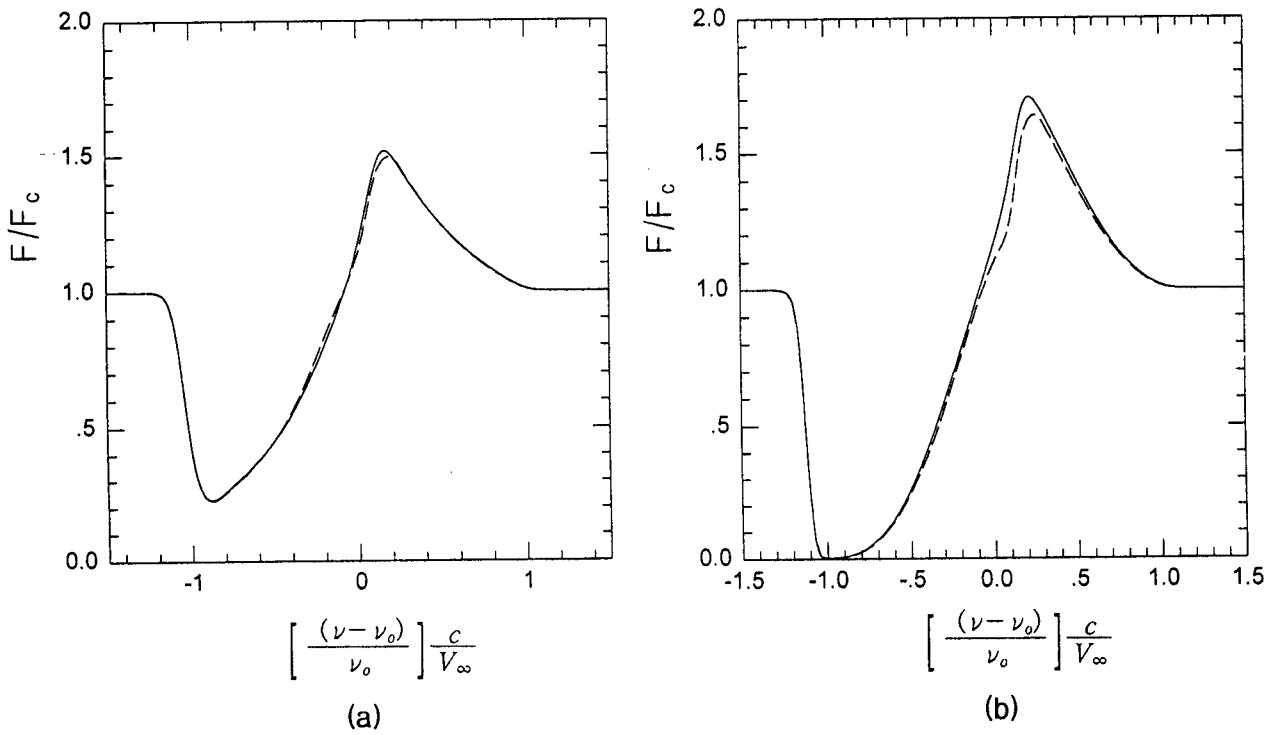

Fig. 5. Normalized flux profiles versus normalized frequency. Correct line profile (solid line), and Sobolev line profile (dashed line). (a) with $\Gamma = 10$, $K_o = 1$, $\beta = 0.5$; (b) with $\Gamma = 10$, $K_o = 10$, $\beta = 0.5$.

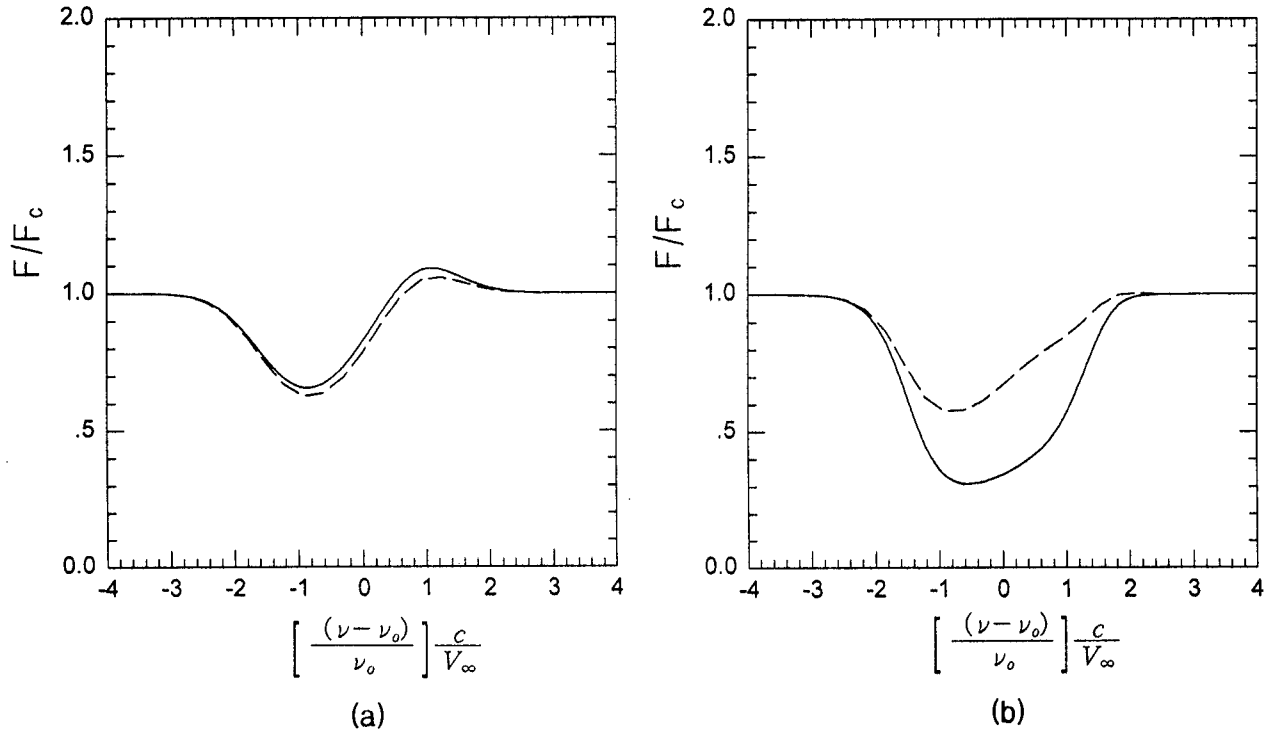

Fig. 6. Normalized flux profiles versus normalized frequency. Correct line profile (solid line), and Sobolev line profile (dashed line). (a) with $\Gamma = 1$, $K_o = 1$, $\beta = 0.5$; (b) with $\Gamma = 1$, $K_o = 1$, $\beta = 2$.

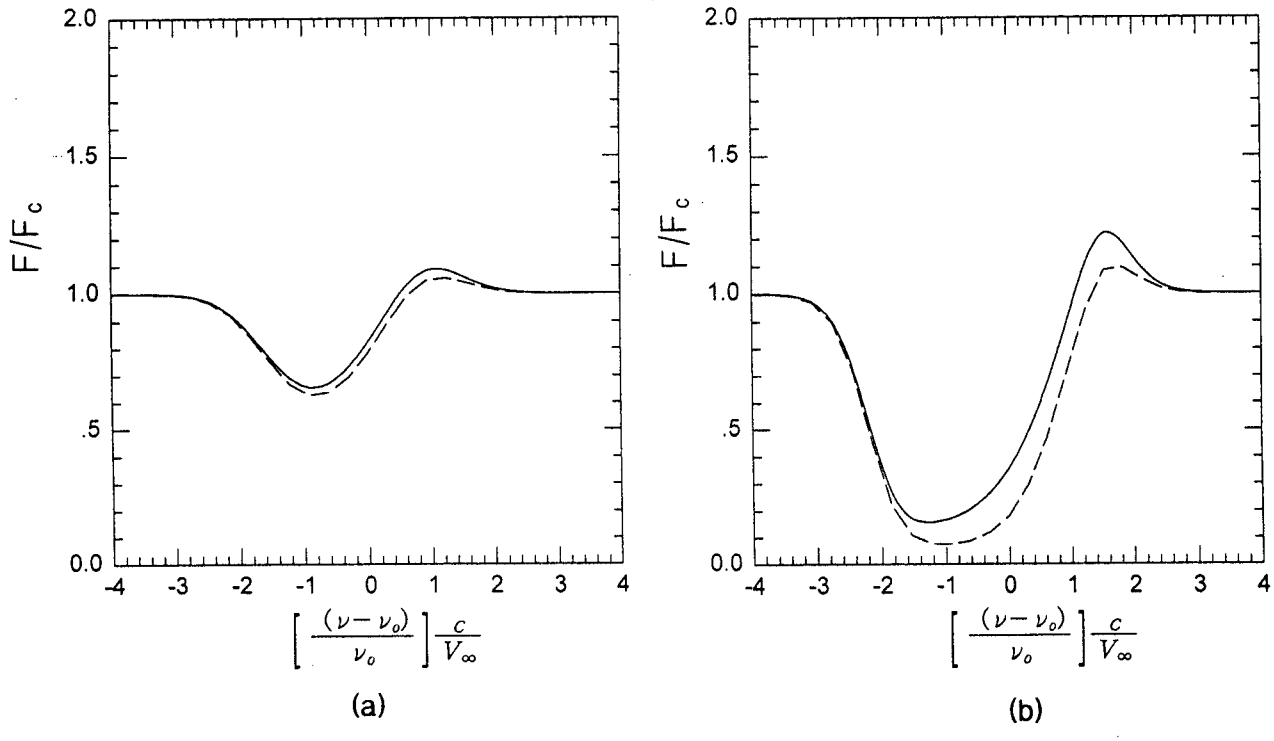

Fig. 7. Normalized flux profiles versus normalized frequency. Correct line profile (solid line), and Sobolev line profile (dashed line). (a) with $\Gamma = 1$, $K_o = 1$, $\beta = 0.5$; (b) with $\Gamma = 1$, $K_o = 10$, $\beta = 0.5$.

(a) Relation of Fit Parameters to Mass Loss Rate

By the fit procedure, the parameters K_o were obtained, which contain the information about the number density of the absorbers, and, therefore, about the mass loss rate and the ionization conditions. From Eq(28)

$$K_o = \frac{\pi e^2}{m_e c} f\lambda \frac{n_k(R_c)}{V_\infty} \frac{V(R_c)/V_\infty}{q(R_c)} R_c \tag{30}$$

Furthermore, n_k is related to the mass density via the excitation fraction of the considered absorbers labelled k of the ion i ; $\frac{n_k}{n_i}$, the ionization fraction of the ion i of element x ; $\frac{n_i}{n_x}$, and the elements abundance ; $\frac{n_x}{n_H}$ by

$$n_k(R_c) = \frac{\dot{M}}{4\pi {R_c}^2 V(R_c)} \frac{1}{\bar{m}} \frac{n_x}{n_H} \frac{n_i}{n_x} \frac{n_k}{n_i} \tag{31}$$

$\bar{m}$ is the mean mass per hydrogen atom, for which we have adopted $\bar{m} = 1.42 m_H$ (solar mixture). Substituting eq(31) into eq(30), we obtain

$$K_o = \frac{\pi e^2}{m_e c} f\lambda \frac{\dot{M}}{4\pi {R_c}^2 {V_\infty}^2} \frac{1}{\bar{m}} \frac{n_x}{n_H} \frac{n_i}{n_x} \frac{n_k}{n_i} \frac{R_c}{q(R_c)} \tag{32}$$

Since in the expanding envelope, practically all ions are in the ground state, we have assumed that $n_k = n_i$, and for definiteness we have set $q(R_c) = 1$. Finally we obtain

$$K_o = \frac{\pi e^2}{m_e c} f\lambda \frac{\dot{M}}{4\pi {R_c}^2 {V_\infty}^2} \frac{1}{\bar{m}} \frac{n_x}{n_H} \frac{n_i}{n_x} R_c \tag{33}$$

(b) The Profile Fitting

Fitting the line profiles, Choe, *et al.*(1996) have a problem that the observed and calculated lines do not match well each other at short wavelength, because the resonance CIV, NV lines consist of two components, which are doublets. In this paper, these lines are treated as doublets. But we could not explain the region where the two components of a doublet overlap. The profiles for ζ Pup were computed with the analytic velocity field with $\beta = 0.5$ (see eq(29)). For the physical parameters of ζ Pup, we refer to Lamers & Morton(1976). Then we have used $R_c = 1.41 \times 10^{12}\, cm$, $V_\infty = 2400$ km/s. For the value of V_∞, we have taken 2400 km/s instead of 2660 km/s. Because the terminal velocity in Lamers & Morton(1976) involves macroscopic turbulent velocity as well as expanding velocity, while in our study, it contains only macroscopic expanding velocity. So, considering the macroscopic turbulent velocity(we have adopted 120 km/s for the value of V_{sto}), the value of V_∞ in our study becomes 2520 km/s. The additional fit parameters compiled in Table 1.

For the physical parameter of τ Sco, we refer to Hamann(1981). Then we have used $R_c = 4.5 \times 10^{11}\, cm$ and $V_\infty = 1600$ km/s. The fit parameters are listed Table 2, and we have used Hamann's empirical three zonal model(see table 3.).

The calculated profiles are compared with the observations in Figure 8. and in Figure 9. In the case of ζ Pup, both the ALI and the Sobolev have given good agreements with the observed line profile. But for the τ Sco, as we have predicted in former chapter, Sobolev approximation has failed within a few Doppler widths from the line center λ_o. This is result from the gradual velocity gradient in the τ Sco.

Table 1. Fit parameters of ζ Pup (adopted by Lamers & Morton, 1976 and Hamann, 1980)

ion	λ (Å)	g	f	log (n_x/n_H)	log (n_i/n_x)	$\dot{M}$($M_\odot$/yr)	V_{sto}(km/s)
CIV	1548.188	2	0.194	-3.43	-1.79	7.9×10^{-6}	~120
	1550.762	2	0.097				

Table 2. Fit parameters of τ Sco (adopted by Hamann, 1981)

ion	λ (Å)	g	f	log (n_x/n_H)	log (n_i/n_x)	$\dot{M}(M_\odot/yr)$	V_{sto}(km/s)
CIV	1548.188	2	0.194	-3.43	-1.79	7.9×10^{-6}	~120
	1550.762	2	0.097				

Table 3. The empirical three zonal model of τ Sco (adopted by Hamann, 1981)

	Zone I	Zone II	Zone III
Velocity range (km/s)	0.01 ..... 0.1	0.1 1000	1000 1600
velocity gradient $\frac{dv}{dr}$	?	2500 km/s/R_c	500 km/s/R_c
Micro turbulence	100 km/s	100 km/s	?
Mass loss rate	$\dot{M} = 1.3 \times 10^{-9}$ $M_\odot$/yr		
q(r)		1	<0.2

For τ Sco-like stars, only ALI method can give the reasonable fit.

VI. CONCLUSIONS

In order to check the validity of Sobolev approximation which can be adopted to a supersonic wind, we have compared the line profiles calculated with both the Sobolev approximation and the ALI method. This comparison shows that Sobolev approximation is not valid any more in the low velocity ratio, Γ, and even at a large Γ if the envelope of a star has the velocity with the gradual gradient near the surface of a star.

The observed UV resonance lines of ζ Pup are satisfactorily reproduced by both the Sobolev approximation and ALI method. But in the case of the τ Sco, the high turbulence velocity has caused the breakdown of the Sobolev approximation for the central part of the line profiles.

We have assumed that a doublet can be treated with a extended two-level problem. But we could not predict the region of a line profile where the two components of a doublet overlap. In order to deal with doublets satisfactorily, we should modify the ALI code.

ACKNOWLEDGEMENTS

The present study was supported by the Basic Science Research Institute Program, Ministry of Education 1996. Project No. BSRI-96-5408.

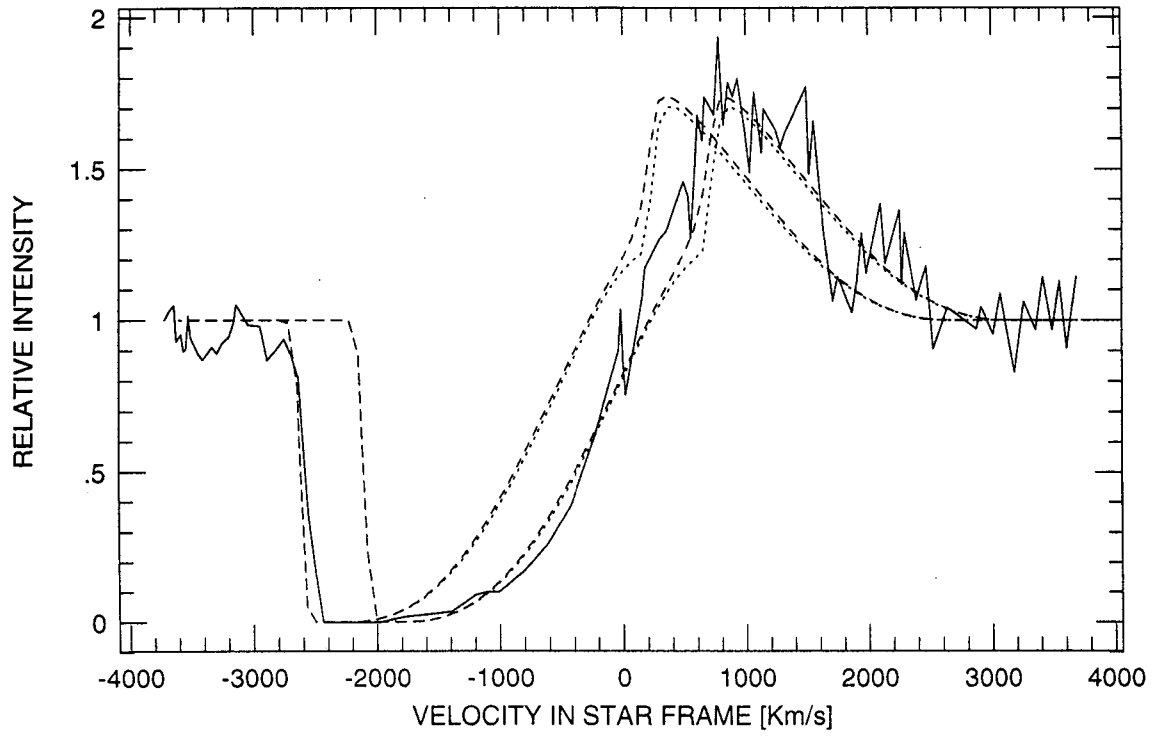

Fig. 8. Copernicus tracing of the CIV resonance line of the ζ Pup (solid line) and theoretical profiles calculated with ALI (dashed line), and Sobolev approximation (dotted line).

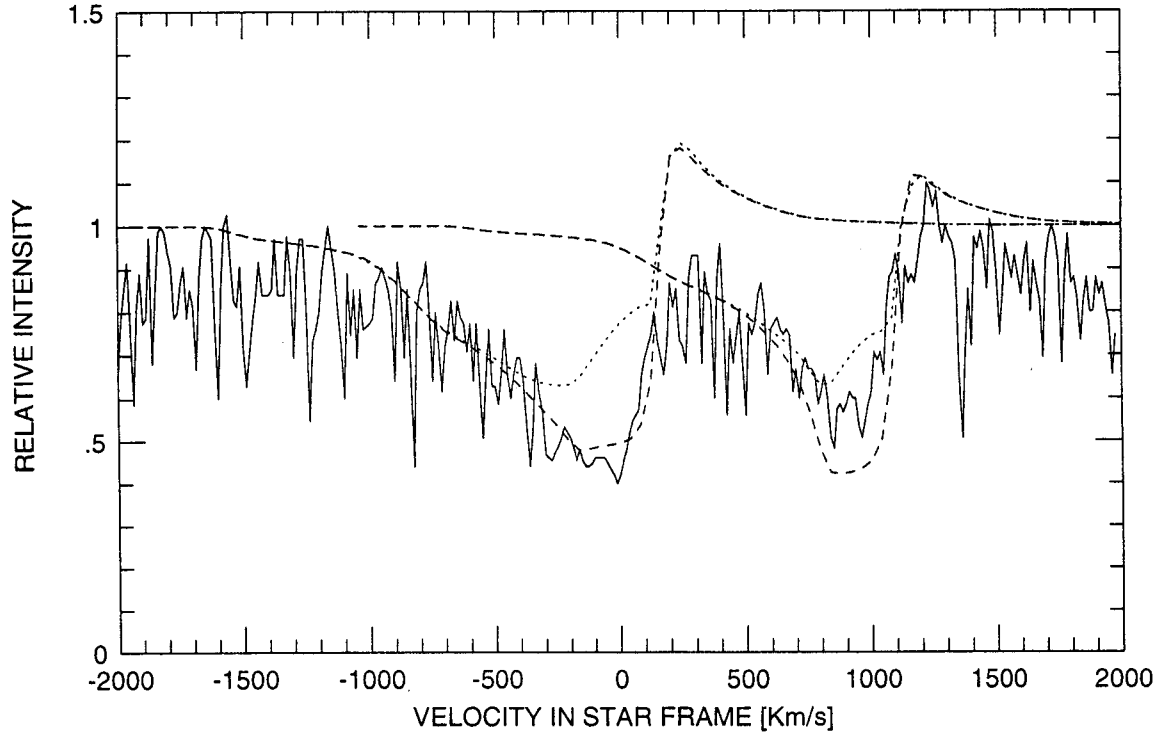

Fig. 9. Copernicus tracing of the NV resonance line of the τ Sco (solid line) and theoretical profiles calculated with ALI (dashed line), and Sobolev approximation (dotted line).

REFERENCES

Cannon, C.J., 1985, The transfer of spectral line radiation, Cambridge University, Camgridge
Castor, J.I., 1970, M.N.R.A.S., 149, 111
Castor, J.I., Abbott, D.C., and Klein, R.I., 1975, ApJ, 195, 157
Choe, S.-U., Kang, M.-Y. and Kim, K.-M., 1996, JKAS, 29(2), 93
Hamann, W.-R., 1980, A&A, 84, 342
Hamann, W.-R., 1981, A&A, 100, 169
Lamers, H.J.G.L.M. and Morton, D.C., 1976, ApJ, Supple, 32, 715
Lamers, H.J.G.L.M. and Rogerson, J.B., 1978, A&A, 66, 417
Morton, D.C and Underhill, A.B., 1977, ApJ, Supple, 33, 83
Rybicki, G.B., and Hummer, D.G., 1978, ApJ, 219, 654
Rybicki, G.B. and Hummer, D.G., 1991, A&A, 245, 171
Schönberg, K., 1985, A&A, 148, 405